第 28 卷第 8 期
2012 年 8 月

无 机 化 学 学 报
CHINESE JOURNAL OF INORGANIC CHEMISTRY

Vol.28 No.8
1729-1735

吲哚乙酸及邻菲啰啉的锌(Ⅱ)配合物的晶体结构及荧光性质

任宜霞* 唐 龙 武玉飞 王丹军 吴亚盘 付 峰
(延安大学化学与化工学院,陕西省化学反应工程重点实验室,延安 716000)

摘要: 利用 3-吲哚乙酸(IAA)、邻菲啰啉(*o*-phen)和氯化锌在水–乙醇体系合成了一种金属配合物[Zn(IAA)$_2$(*o*-phen)] (**1**),并对其进行了 X-射线单晶衍射分析、热重分析、元素分析、红外光谱、紫外光谱、荧光光谱表征。结构分析表明,该配合物中,锌离子处于四配位的四面体构型中,分别与 2 个 IAA 阴离子的羧基氧原子及 1 个邻菲啰啉的 2 个氮原子配位。通过超分子作用力:氢键和面对面式的 $\pi\cdots\pi$ 堆积作用力的自组装作用使这些分子形成二维的超分子层结构, 继而这些层层间通过边对面式的 $\pi\cdots\pi$ 堆积作用力进一步的组装成三维的超分子结构。热重分析显示,该配合物具有较高的热稳定性。配合物的液态及固体荧光性质研究表明,此配合物具有一定荧光性质。

关键词: 锌配合物; 晶体结构, 荧光性质
中图分类号: O614.24$^+$1 **文献标识码**: A **文章编号**: 1001-4861(2012)08-1729-07

Structural Analysis and Photoluminescence Properties of a Discrete Zinc (Ⅱ) Complex with 3-Indoleacetic Acid and Phenanthroline

REN Yi-Xia* TANG Long WU Yu-Fei WANG Dan-Jun WU Ya-Pan FU Feng
(*College of Chemistry and Chemical Engineering, Shaanxi Key Laboratory of Chemical Reaction Engineering, Yan'an University, Yan'an, Shaanxi* 716000, *China*)

Abstract: A Zn(Ⅱ) complex, [Zn(IAA)$_2$(*o*-phen)] (**1**) (IAA=3-indoleacetic acid, *o*-phen=1,10-phenanthroline), was synthesized and characterized by single crystal X-ray diffraction, TGA analysis, elemental analysis, IR, UV-vis and luminescence spectroscopy. For complex **1**, each $Zn^{Ⅱ}$ ion is in the tetra-coordinated tetrahedral geometry from two mono-dentated IAA anions and one chelated o-phen ligand. The H-bonds and the face-to-face $\pi\cdots\pi$ stacking interactions assemble 2D supramolecular layer-structure, then via the edge-to-face C–H$\cdots\pi$ stacking interactions the 2D layers are constructed into 3D supramolecular structure. The TG analysis shows the complex possesses a high thermal stability. The solution and solid-state photoluminescence of **1** are presented. CCDC: 819169.

Key words: zinc(Ⅱ) complex; crystal structure; solution and solid-state photoluminescence

0 Introduction

The investigation of supramolecular chemistry has attracted extensive attention in the field of chemistry for its importance in molecular recognition and host-guest chemistry since J. M. Lehn defined it[1-3]. In designing and synthesizing the metal-organic supramolecular complexes, the selection of organic ligand is one of key factors we mainly considered. We usually select the multi-coordinated ligands containing

收稿日期:2011-12-06。收修改稿日期:2012-04-01。
国家自然科学基金(No.21003103)及陕西省教育厅科技项目(No.12JK0609)资助项目。
*通讯联系人。E-mail:renyixia1@163.com;会员登记号:S06N9633M1003。

phenyl or pyridine rings to meet our desires for forming weak intermolecular forces, such as H-bonds, weak non-covalent interactions, π stacking interactions and so on[4-7]. As reported in references, the existence of kinds of supramolecular interactions may influence the luminescent, magnetic or adsorption properties of metal-organic complexes[8-10]. 3-Indoleacetic acid (IAA) is not only an excellent growth hormone, but a good π-conjugated organic ligand because that the indole ring benefits to form π stacking interactions and the nitrogen atom of the ring may favor the formation of H-bonds. Although many works about the metal complexes with IAA have been reported, mainly relating to their synthesis, spectrum and bioactivity, several crystal structures of IAA complexes have been published[11-13]. Moreover, we introduce the evergreen N-donor ligand, 1,10-phenanthroline, to form π stacking interactions and alter the dimension of the supramolecular structure. In this paper, we prepared a Zn(Ⅱ) supramolecular complex with IAA and *o*-phen ligands, and investigated its crystal structure, IR spectroscopy, thermal stability and luminescence properties in EtOH solution and solid-state.

1 Experimental

1.1 Materials and methods

All chemicals were commercially available and used as received without further purification. Elemental analyses (CHN) were performed using an Vario EL elemental analyzer. FT-IR spectra were recorded from KBr pellets in the range of 4 000~400 cm^{-1} on a Nicolet Avatar 360 FT-IR spectrometer. Thermogravimetric curves were measured on a Mettler (USA) at a heating rate of 10 ℃·min^{-1} from room temperature to 1 000 ℃ in air. Fluorescence measurements were carried out with a SHIMADZU RT5301PC spectrofluorophotometer. UV-Vis absorption experiments were performed on a SHIMADZU UV 2500PC spectrometer equipped with an integrating sphere for diffuse-reflectance spectroscopy, and the spectra were collected in the 200~800 nm range at room temperature. The phase of as-synthesized products was determined by X-ray diffraction (XRD) using a SHIMADZU XRD-7000 X-ray differactometer with Cu $K\alpha$ radiation (λ=0.154 06 nm). The simulated PXRD patterns were obtained from the single-crystal X-ray diffraction data.

1.2 Computational details

All calculations have been processed in Gaussian 03 package[14]. The geometries optimization were carried out with the hybrid DFT method on the basis of B3LYP functional[15-16]. The magnetic isotropic shielding tensors were also calculated using B3LYP/6-31G (d) approach. The experimentally determined geometry for the complete structure of complex **1** was used for the calculation of the magnetic exchange coupling constants. Neither variation of the geometrical parameters nor the geometry optimization[17] was attempted in this calculation because a small variation in the geometry can have a big effect on the calculated magnetic interaction parameters.

1.3 Synthesis

A hartshorn solution (20 mL) containing $ZnCl_2$ (1 mmol, 0.136 g) was added dropwise into an absolute alcohol stirring solution (20 mL) of IAA (2 mmol, 0.350 g), then 20 mL solution of KCl (1 mmol, 0.075 g) and 20mL ethanol solution of *o*-phen (0.5 mmol, 0.101 g) were added continually to the mixture solution. At 45 ℃, the mixture solution was stirring for one hour, filtered and placed quietly in the air. After two weeks, several brown block crystals are collected (70% yield based on Zn). Anal. Calcd. for $C_{20}H_{17}Cl_2N_3O_8Zn$ (%): C, 64.71; H, 4.07; N, 9.43. Found(%): C, 64.67; H, 4.28; N, 9.50. IR (KBr, cm^{-1}): 3 395(w), 3 170(w), 3 057(w), 2 925(w), 2 873(w), 1 594.6 (s), 1 518.9(m), 1 457.9(m), 1 426.5(s), 1 400(m), 1 380.8 (m), 1 230(w), 1 101(w), 845.5(s), 745(s),723(s).

1.4 Crystal structure determination

Single crystal X-ray diffraction analysis of complex **1** was carried out on a Bruker SMART APEX CCD diffractometer equipped with a graphite monochromated Mo $K\alpha$ radiation (λ=0.071 073 nm). The collected data were reduced with the SAINT program[18]. The structure was solved by direct methods with SHELXS-97 and refined by full-matrix least-squares on F^2 using SHELX-97[19]. An empirical absorption correction was applied with the program

Table 1　Crystallographic data for complex 1

Empirical formula	$C_{32}H_{24}N_4O_4Zn$	$F(000)$	1 224
Formula weight	593.92	Crystal size / mm	0.23×0.17×0.17
Temperature / K	296(2)	θ range for data collection / (°)	2.40 to 27.61
Wavelength / nm	0.071 073	Index range	$-16 \leqslant h \leqslant 13, -16 \leqslant k \leqslant 14, -14 \leqslant l \leqslant 22$
Crystal system	Monoclinic	Reflections collected	15 098
Space group	$P2_1/c$	Reflections unique (R_{int})	5 995 (0.045 5)
a / nm	1.230 6(13)	Completeness to θ=28.26° / %	98.50
b / nm	1.256 2(13)	Refinement method	Full-matrix least-squares on F^2
c / nm	1.766 8(18)	Data / restraints / parameters	5 995 / 0 / 370
β / (°)	105.97	Goodness-of-fit on F^2	1.002
Volume / nm^3	2.6258(5)	Final R indices ($I>2\sigma(I)$)	R_1=0.041 1, wR_2=0.080 9
Z	4	R indices (all data)	R_1=0.084 6, wR_2=0.093 3
Calculated density / (g·cm^{-3})	1.502	Largest diff. peak and hole / (e·nm^{-3})	269 and −297
Absorption coefficient / mm^{-1}	0.983		

SADABS[20]. All non-hydrogen atoms were refined anisotropically. The hydrogen atoms were set in calculated positions and refined by a riding mode. The crystallographic details of complex **1** are provided in Table 1, and the selected bond distances and angles are listed in Table 2, respectively.

CCDC: 819169.

Table 2　Selected bond lengths (nm) and bond angles (°) for 1

Bondlengthandangle	Experiment	Calculationa
Zn(1)-N(1)	0.208 4(2)	0.216 19
Zn(1)-N(2)	0.209 2(2)	0.216 19
Zn(1)-O(1)	0.196 2(2)	0.203 69
Zn(1)-O(4)	0.195 7(2)	0.203 65
O(4)-Zn(1)-N(2)	114.44(8)	112.375 5
O(1)-Zn(1)-N(2)	105.51(7)	103.597 8
O(4)-Zn(1)-O(1)	129.94(7)	127.563 6
N(1)-Zn(1)-N(2)	80.73(8)	78.298 8
O(4)-Zn(1)-N(1)	107.92(7)	105.543 3
O(1)-Zn(1)-N(1)	107.14(7)	105.612 7

[a] Bond lengths and angles calculated by DFT methods at B3LYP/6-31G(d) level.

2　Results and discussion

2.1　Crystal structure

Single-crystal X-ray crystallographic studies reveal that compound **1** crystallizes in a monoclinic space group $P2_1/c$, which is made up of mononuclear tetra-coordinated Zn units by a great deal of supramolecular interactions. In the asymmetry unit, there are one $Zn^{Ⅱ}$ ion, two IAA anions and one *o*-phen molecule (Fig.1). In order to distinguish the two IAA ligands, we labeled IAA(a) (based on C15 to C22 and N3) and IAA (b) (based on C24 to C32 and N4). For each mononuclear unit, the $Zn^{Ⅱ}$ ion tetrahedrally coordinated by O2 and O4 of two IAA ligands and N1 and N2 of *o*-phen molecule forms a slightly distorted tetrahedron coordination geometry. Both two IAA^- anions act as monodentate ligands through one oxygen atoms of carboxyl group, and the nitrogen atom of pyridine ring doesn't participate in coordinating to Zn atom. The mean Zn-O bond length is 0.195 9 nm, and the mean Zn-N bond length is 0.208 8 nm, all of which are accordant with the normal reported Zn-O and Zn-N bond lengths[21-24].

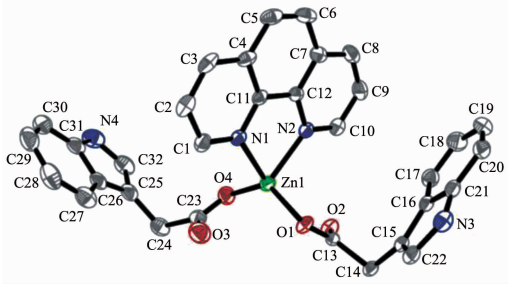

Fig.1　Molecular structure of complex **1** with an ellipticity of 30%; All the hydrogen atoms are omitted for clarity

Two kinds of hydrogen bonding interactions between N atoms and O atoms of different IAA (a)

Table 3 $\pi\cdots\pi$ stacking interactions of complex 1

Type	Ring(*i*) to ring(*j*)	Centroid separation Cg-Cg / nm	Dihedral angle (*i*,*j*) / (°)	Perp. distance between rings / nm
face-to-face	o-phen to IAA(a)			
	R(1) to R(2)^{I}	0.3784	0	0.3374
face-to-face	o-phen to o-phen			
	R(1) to R(3)^{II}	0.359 7	0	0.338 5
Type	Atom to ring(*j*)	Centroid separation H-Cg / nm	Angle (CHCg) / (°)	Perp. distance between rings / nm
edge-to-face	C3-H3···IAA(a)			
	C3 to R(2)	0.381 6		0.333 1
	H3 to R(2)	0.328 1	118.7	0.262 5
edge-to-face	C6-H6···IAA(b)			
	C6 to R(4)^{III}	0.377 4		0.355 5
	H6 to R(4)^{III}	0.297 5	144.9	0.274 3

Symmetry operations: ^{I} x, 0.5−y, −0.5+z; ^{II} 1−x, −y, −z; ^{III} −1+x, y, z; Ring (1): C4-C5-C6-C7-C12-C11; Ring (2): C16-C17-C18-C19-C20-C21; Ring(3): C1-C2-C3-C11-C4-N1; Ring(4): C26-C27-C28-C29-C30-C31.

ligands (N3−H3A···O2^{I}: 0.288 nm, the angle is 175.8° and N4−H4A···O1^{II}: 0.300 nm, the angle is 110.6°, the symmetry operations: ^{I} 1−x, −0.5+y, 0.5−z; ^{II} x, 0.5−y, −0.5+z) extend these mononuclear Zn(Ⅱ) molecules into 2D supramolecular structure. Furthermore, the dihedral angle between *o*-phen ring and IAA (a) is 54.8°, while that between *o*-phen ring and IAA (b) is 118.9°. The gap between the two dihedral angles results into different supramolecular arrangement for complex **1**: IAA (a) molecules and *o*-phen ligands play key roles in 2D supramolecular construction in bc plane via $\pi\cdots\pi$ stacking interactions (table 3). Interestingly, the face-to-face stacking types between two adjacent *o*-phen ligands (the distance is 0.339 nm) from two molecules, between *o*-phen and IAA (a) (the distance is 0.357 nm), assembled into a quaternion-packing unit in an IAA(a)···*o*-phen···*o*-phen···IAA(a) order (Fig.2). As the edges of grid, the quaternion-packing units intervein into 2D network with the intersections by the edge-to-face $\pi\cdots\pi$ stacking interactions from C3−H3···IAA(a) (the distance of C3 to Cg is 0.333 nm) (Fig.3). Both hydrogen bonding and π-π stacking interactions reinforce the stability of 2D supramolecular layer. These 2D supramolecular layers construct three-dimension supramolecular structure through the edge-to-face C−H···π stacking interactions from C6-H6 atoms of *o*-phen ligands and

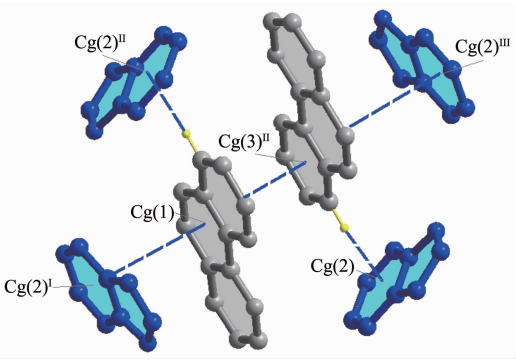

Cg (1): C4-C5-C6- C7-C12-C11; Cg (2): C16-C17-C18-C19-C20-C21; Cg(3): C1-C2-C3-C11-C4-N1; Symmetry operations: ^{I} x, 0.5−y, −0.5+z; ^{II} 1−x, −y, −z; ^{III} −1+x, −0.5+y, 0.5−z; IAA (b) ligands and Zn, O, H atoms are deleted for clarity

Fig.2 Illustration for a quaternion-packing unit in an IAA(a)···*o*-phen···*o*-phen···IAA(a) order

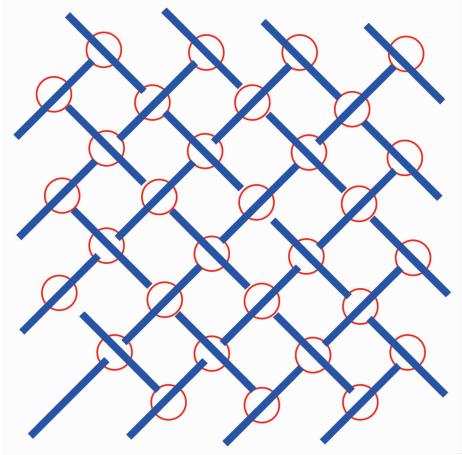

■ represents one unit of [IAA(a) ···*o*-phen···*o*-phen···IAA(a)] π stacking interactions; ○ represents edge-to-face π stacking interactions

Fig.3 Structural model for 2D grid layers based on quaternion-packing unit in complex **1**

the IAA(b) ligands (the distance of C6–H6···IAA(b) is 0.355 nm).

2.2 IR spectroscopy

The IR spectrum of complex **1** exhibits one sharp middle peak at 3 395.1 cm^{-1}, which is assigned to the $\nu_{N\text{-}H}$ stretching vibration and decreased compared with the free IAA ligand for the existence of hydrogen bonds (N3–H3A···O2 and N4–H4A···O1)[25]. The bands at 1 594 and 1 426 cm^{-1} are the ν_{COO^-} stretching vibration and indicate the coordination of carboxyl group to Zn(Ⅱ) for the large red-shift compared with the IR spectrum of free ligand IAA. Furthermore, the band at 745.2 cm^{-1} stems from four neighboring hydrogen atoms on phenyl ring. The analysis of IR spectrum of the complex is in agreement with its crystal structure and charge balance consideration.

2.3 Thermogravimetric analyses

Thermalgravimetric analyses were performed on **1** in air from 30 to 1 000 ℃ (Fig.4). The TGA curve showed two steps of weight losses. The first weight loss is 69.61% from 311 to 480 ℃ and corresponds to the loss of one *o*-phen molecule (calcd. 69.32%). The second weight loss from 480 to 1 000 ℃ is only up to 53.13% and it is obvious that the process didn′t finish due to the limited measure scope of the thermogravimetric analyzer. But the fact reveals the high thermal ability of complex **1** owing to a great deal of supramolecular interactions, which is accorded with the result of structural analysis of **1**.

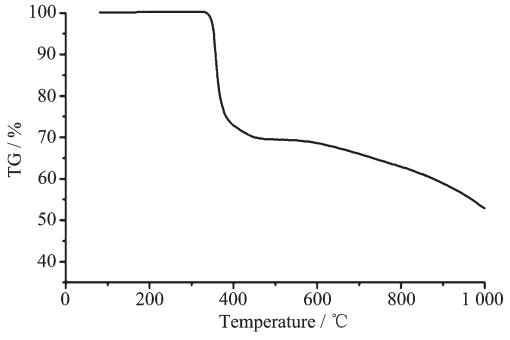

Fig.4　TG curve of the complex **1**

2.4 Theoretical calculation

Optimized geometry structure: The data of the main bond lengths and bond angles for **1** in the optimization structure are showed in Table 2. The monomer [Zn(IAA)$_2$(o-phen)] of **1** was optimized by the DFT method with the B3LYP functional. The Zn-O and Zn-N bond length calculated are slightly longer than those experimental values, and the $\Delta_{cal.\text{-}exp.}$ (the difference between calculated and experimental values) of bond lengths ranges from 0.006 9 to 0.007 9 nm. The highest deviation is about 2.5° for the bond angles in complex **1**. There is a little deviation between the calculation and the experimental values. The reason of the deviation is maybe as follows: the approximation of calculation methods and basis set, the neglect of anionic effect in the course of calculation and the chemical environmental difference of the complex. The deviation can be accepted in theoretical calculation for a big system.

Energies and components of molecular orbitals: The energy of the title complex is −1 806.208 234 a.u. after 12 cycles of calculation with HOMO energy of −0.272 24 a.u. (alpha electrons), LUMO energy 0.060 07 a.u. (alpha electrons), and the band gap 0.332 31 a.u. (9.04 eV), indicating that this configuration is stable.

2.5 Luminescent properties

To investigate the potential properties of **1**, we measured the fluorescent spectra of complex **1**, free IAA and *o*-phen ligands in EtOH solution and the solid state at ambient temperature. Complex **1** exhibits photoluminescence both in EtOH solution and in the solid state (Fig.5). As shown in Fig.5 (a), the free ligands IAA and *o*-phen themselves are luminescent compounds with 390 nm (λ_{ex}=290 nm) and 402 nm (λ_{ex}=307 nm) in the EtOH solution, respectively, which are dominated by π-π* type of fluorescence. In the solution state, two emission peaks of complex **1** feature a stronger peak at 497 nm and a weaker one at 400 nm upon excitation at 308 nm. The broad emission at 400 nm could be assigned to the π-π* transition of both IAA and *o*-phen because the similar peaks have been observed around 400 nm for them. The stronger emitting peak at 497 nm is neither metal-to-ligand charge transfer (MLCT) nor ligand-to-metal transfer (LMCT) in nature, since the Zn(Ⅱ) ions with d^{10} configuration are difficult to oxidize or reduce, which can be attributed to the ligand-centered emission[26-28].

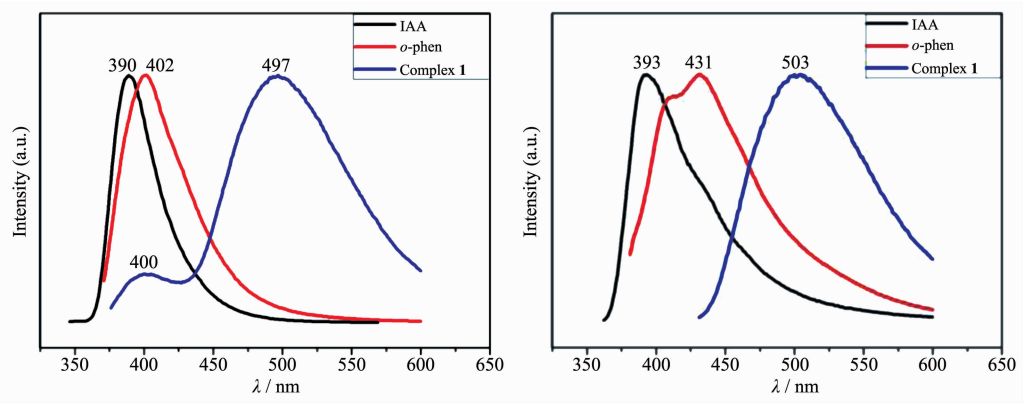

Fig.5 Normalized fluorescence spectra for complex **1** and free ligands IAA and *o*-phen (a) in EtOH solution and (b) in the solid state at room temperature

Therefore, it may be assigned to the π-π* intraligand fluorescence. The large red-shifted of the emission at 497 nm for complex **1** could be attributed to the replacement of hydrogen proton of the carboxyl group of IAA by Zn(Ⅱ) ion, which decreases its π*-*n* or π*-π gap and results in the red-shift of the emission peak[29-30]. So, the emission at 497 nm could be assigned to the coordination of IAA ligands and the chelating of *o*-phen molecules.

In the solid-state, one broad emission peak at 503 nm (λ_{ex}=330 nm) may be attributed to mixed ligand-centered, which is 6 nm red-shifted compared to the emission in EtOH solution (Fig.5b). It can be explained that the cooperative effect of diverse weak interactions controlled by $\pi\cdots\pi$ stacking and hydrogen bonds play an essential role to decrease the HOMO-LUMO energy gaps[31-32].

In order to confirm the phase purity of the bulk materials of **1**, powder X-ray diffraction (PXRD) patterns were recorded at room temperature (Fig.6). Compared to the simulated patterns from the single crystal data, we could conclude that the bulk as-synthesized crystalline materials represent complex **1** due to their adequate similarity.

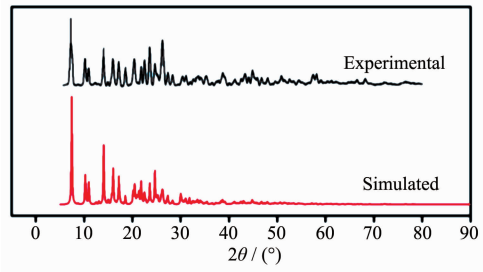

Fig.6 PXRD patterns for **1**

2.6 UV-Vis reflectance spectroscopy

The UV-Vis absorption spectra of complex **1** and the free ligands were recorded in reflectance mode in the EtOH solution and the solid state at room temperature (Fig.7). From the spectra in both the EtOH solution and the solid state, we found the absorption spectra of complex **1** are similar to those of free ligands, so their absorption bands can be

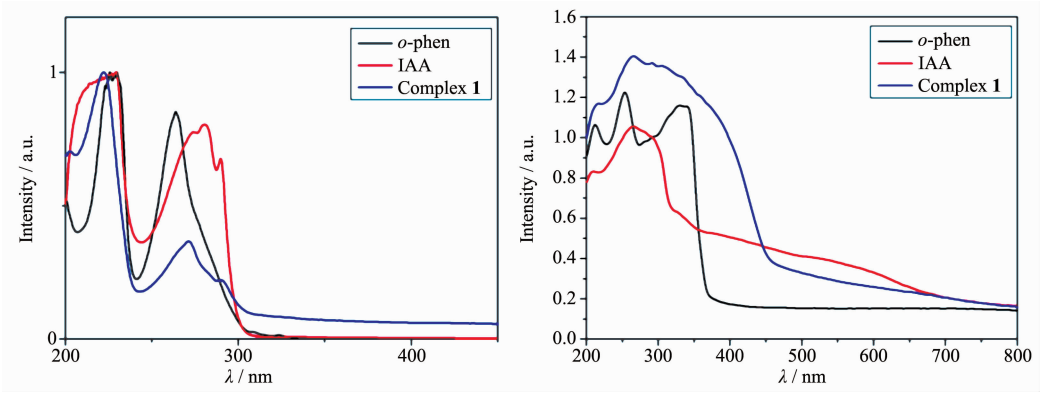

Fig.7 UV-Vis reflectance spectra of complex **1** and free ligands in (a) EtOH solution and (b) solid-state

assigned to the intraligand π-π* transitions of the ligands. The results are accorded with the analysis of luminescent spectra of complex **1** and free ligands.

3 Conclusions

A new Zn(Ⅱ) complex with IAA and N-donor chelated (*o*-phen) ligands has been prepared under mild conditions. The crystal structure of **1** indicates that the geometries and sizes of the organic ligands IAA and *o*-phen, which provide potential supramolecular recognition sites for H-bonds and π stacking interactions, are essential in assembling of the supramolecular structure. The studies on the thermal stability of **1** reveal that the complex decomposes from a high temperature of 311 ℃ for the structural reason. The photoluminescence in EtOH solution and the solid state indicate that it may be good candidates for luminescent materials.

References:

[1] Lehn J M. *Angew Chem. Int. Ed.*, **1988**,**27**:89-112

[2] Jiao D Z, Biedermann F, Tian F, et al. *J. Am. Chem. Soc*., **2010**,**132**:15734-15743

[3] Hoeben F J M, Jonkheijm P, Meijer E W, et al. *Chem. Rev*., **2005**,**105**:1491-1546

[4] Seko H, Tsuge K, Igashira-Kamiyama A, et al. *Chem. Commun*., **2010**,**46**:1962-1964

[5] Mir M H, Vittal J J. *Angew. Chem. Int. Ed.*, **2007**,**46**:5925-5928

[6] Li J R, Timmons D J, Zhou H C. *J. Am. Chem. Soc*., **2009**, **131**:6368-6369

[7] Jia J H, Blake A J, Champness N R, et al. *Inorg. Chem*., **2008**,**47**:8652-8664

[8] Roubeau O, Clérac R. *Eur. J. Inorg. Chem*., **2008**:4325-4342

[9] Lightfoot M P, Mair F S, Gritchard P R, et al. *Chem. Commun*, **1999**,**19**:1945-1946

[10]Kitaura R, Seki K, Akiyama G, et al. *Angew. Chem. Int. Ed.*, **2003**,**42**:428-431

[11]HUANG Zhong-Le(黄种乐), YU Xiu-Fang(余秀芬). *Chin. J. Struct. Chem.*(*Jiegou Huaxue*), **1988**,**7**:130-132

[12]Masuda H, Sugimori T, Odani A, et al. *Inorg. Chim. Acta*., **1991**,**180**:73-79

[13]ZHANG Hong(张宏), PENG Jin-Hua(彭金华), SONG Zhi-Gang(宋之刚), *J. Northwest Nor. Univ*.: *Nat. Sci. Edi.*(*Xibei Shifan Daxue Xuebao*), **2001**,**37**:63-66

[14]Frisch M J, Trucks G W, Schlegel H B, et al. *Gaussian* 03, Gaussian, Inc., Wallingford CT, **2004**.

[15]Becke A D. *J. Chem. Phys*., **1997**,**107**:8554-8560

[16]Lee C, Yang W, Parr R G. *Phys. Rev. B*, **1988**,**37**:785-789

[17]Ruiz E, Cano J, Alvarez S, et al. *Int. J. Quantum Chem*., **1999**,**20**:1391-1396

[18]Siemens. *SAINT*: *Area Detector Control and Integration Software*, Siemens Analytiacl X-ray Instruments Inc., Madison, WI, USA, **1996**.

[19]Sheldrick G M. *SHELXL*97 and *SHELXTL Software Reference Manual*, Version 5.1, Brucker AXS Inc Madison, WI, USA, **1997**.

[20]Sheldrick G M. *SADABS, Program for Empirical Absorption Correction of Area Detector Data*, University of Göttingen, Germany, **1996**.

[21]Yang G P, Wang Y Y, Liu P, et al. *Cryst. Growth Des*., **2010**,**10**:1443-1450

[22]Yang G P, Wang Y Y, Zhang W H, et al. *CrystEngComm*, **2010**,**12**:1509-1517

[23]Yang F, Ren Y X, Li D S, et al. *J. Mol. Struct*., **2008**,**892**: 283-288

[24]Zhang M L, Li D S, Wang J J, et al. *Dalton Trans*., **2009**: 5355-5364

[25]Yang Y, Zhang W J, Pei S X, et al. *J. Mol. Struct.*:*Theochem*, **2005**,**732**:33-37

[26]Wen L, Li Y, Lu Z, et al. *Cryst. Growth Des*., **2006**,**6**:530-537

[27]Wen L, Lu Z, Lin J, et al. *Cryst. Growth Des*., **2007**,**7**:93-99

[28]Lin J G, Zang S Q, Tian Z F, et al. *CrystEngComm*, **2007**,**9**: 915-921

[29]Zhang L P, Ma J F, Pang Y Y, et al. *CrystEngComm*, **2010**, **12**:4433-4442

[30]Ma J F, Yang J, Li S L, et al. *Cryst. Growth Des*., **2005**,**5**: 807-812

[31]Meng F Y, Zhou Y L, Zou H H, et al. *J. Mol. Struct*., **2009**, **920**:238-241

[32]Yu X Y, Zou H H, Wei L Q, et al. *Inorg. Chem. Commun*., **2010**,**13**:1137-1139